Colloid Polym Sci (2006) 284: 1419–1430
DOI 10.1007/s00396-006-1515-6

ORIGINAL CONTRIBUTION

**M. Larrañaga**
**P. Arruti**
**E. Serrano**
**K. de la Caba**
**P. M. Remiro**
**C. C. Riccardi**
**I. Mondragon**

# Towards microphase separation in epoxy systems containing PEO/PPO/PEO block copolymers by controlling cure conditions and molar ratios between blocks. Part 2. Structural characterization

Received: 15 September 2005
Accepted: 10 April 2006
Published online: 13 June 2006


M. Larrañaga · P. Arruti · E. Serrano · K. de la Caba · P. M. Remiro · I. Mondragon (✉)
Materials+ Technologies Group.
Dpto Ingeniería Química
y M Ambiente, Escuela Univ
Politécnica/Unib Eskola Politeknikoa,
Universidad País Vasco/Euskal Herriko
Unibertsitatea. Pza Europa,
1, 20018
Donostia/San Sebastián, Spain
e-mail: iapmoegi@sc.ehu.es
Tel.: +34-943-017271
Fax: +34-943-017130

C. C. Riccardi
Institute of Materials Science
and Technology (INTEMA),
University of Mar de Plata
and National Research Council
(CONICET),
J. B. Justo 4320-(7600),
Mar de Plata, Argentina

**Abstract** The influence of addition of poly(ethylene oxide)-block-poly (propylene oxide)-block-poly(ethylene oxide) (PEO–PPO–PEO) copolymers on final morphologies of modified epoxy matrices has been investigated as a function of PEO:PPO molar ratio and cure conditions by comparison with the cured epoxy blends only containing poly(ethylene oxide) (PEO) or poly(propylene oxide) (PPO) homopolymers. Atomic force microscopy (AFM) has been used to characterize structural features of blends. Whilst diglycidyl ether of bisphenol-A (DGEBA)/4,4'-diaminodiphenylmethane (DDM)/PPO system macrophase separates, the interactions between PEO and cured epoxy are responsible for miscibility of DGEBA/DDM/PEO system. Depending on PEO:PPO molar ratio, micro- or macrophase separated morphologies have been obtained for block copolymer modified epoxy matrices. Moreover, the influence of both copolymer content and cure temperature on final morphologies has also been investigated by both experimental and theoretical analysis.

**Keywords** Epoxy · Triblock copolymers · Homopolymers · Microphase separation · Thermodynamics

## Introduction

The modification of epoxy resins with block copolymers has been investigated by several authors in recent years [1–10; Larrañaga et al., submitted for publication; 11–13]. Block copolymers are the focus of a great deal of research activity because their intrinsic ability to self-assemble into different structures ordered at nanoscale. One feasible pathway for generating microphase separated thermosetting matrices is the use of amphiphilic block copolymers with one of the blocks miscible with the epoxy resin. Understanding the principles that underlie the development of such morphologies can allow the design of novel nanomaterials in a controlled way.

Recent studies carried out by Ritzenthaler et al. [2, 3] for ABC triblock copolymer/epoxy-diamine blends show that the way to avoid macrophase separation and to obtain microstructured thermoset matrices is to use block copolymers containing a block miscible with the growing matrix during the whole cure reaction process. As reported before [4], though cure conditions are important to obtain micro- or macrophase separated systems, the generation of microphase separated structures is not only a function of block constituents, but also of block ratio.

In the first part of this work (Larrañaga et al., submitted for publication), the influence of PEO:PPO block ratio on cure kinetics of PEO–PPO–PEO modified epoxy systems has been investigated. Different delay on cure kinetics was

observed for systems modified with copolymers having different block ratios. Besides, the cure process was shifted to longer times as block copolymer content or PEO content in the block copolymer increased. Kinetics, together with thermodynamics, is a key factor for controlling the phase separation process. In this second part of the work, we analyse the microstructural features of DGEBA/DDM epoxy matrices modified with three PEO–PPO–PEO block copolymers having different block ratios and molecular weights. The influence of PEO:PPO ratio on final morphologies has been investigated at different cure temperatures and copolymer contents. Systems modified with PEO and PPO homopolymers have also been analysed for better understanding of the influence of PEO:PPO ratio. Thermodynamic analysis has been developed to complete the study. A Flory–Huggins lattice model has been employed to provide a qualitative frame for the discussion.

## Experimental

The characteristics of epoxy matrix components, hydroxyl-terminated PEO–PPO–PEO block copolymers, and the corresponding PEO and PPO homopolymers used are shown in Table 1.

Likewise, PEO–PPO–PEO and homopolymers modified epoxy blends were prepared as described previously [4; Larrañaga et al., submitted for publication]. They were cured in a preheated mould at two different temperatures, 80 °C for 6 h or 140 °C for 3 h, degassing with vacuum during the early stage of cure and then postcured at 190 °C for 2 h, thereafter, allowing them to gradually cool to room temperature.

Fourier transform infrared (FTIR) spectroscopic analysis was performed in a Perkin-Elmer 1,600 PC spectrometer. The solid analyte was mixed with KBr. Spectra were taken with 2 $cm^{-1}$ resolution and 20 scans were carried out from 4,000 to 400 $cm^{-1}$.

Dynamic mechanical behaviour was studied in a Metravib viscoanalyser from 30 to 250 °C at 3 °C/min and 10 Hz using 60×12×5 $mm^3$ samples with a bending device. Constant amplitude of 0.1 V was employed. An initial displacement of 80 μm was applied to ensure contact between sample and geometry.

The morphological features of the blends were investigated by atomic force microscopy (AFM) using a scanning probe microscope (SPM) (Nanoscope IIIa, Multimode from Digital Instruments) operating in tapping mode (TM-AFM) under ambient conditions. Etched silicon probes with a cantilever configuration of single beam and 125 μm of length and a tip with a nominal radius of curvature of 5–10 nm were used.

Transmission Optical Microscopy (TOM) measurements were made using an Olympus BH-2 optical microscope

**Table 1** Characteristics and chemical structures of materials used

| Material | Chemical structure and supplier | Molar mass (g/mol) | Density | PEO:PPO Molar ratio |
|---|---|---|---|---|
| DGEBA | 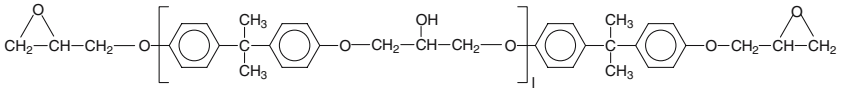 Dow Chemical | 350 | 1.16 | |
| DDM | 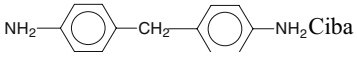 Ciba | 198 | 1.09 | |
| PEO | 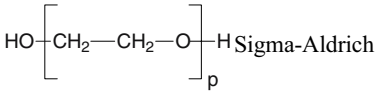 Sigma-Aldrich | $M_w$=8,000 | 1.027 | |
| PPO | 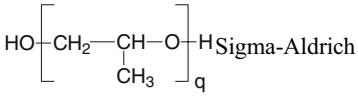 Sigma-Aldrich | $M_w$=2,000 | 1.005 | |
| PEO–PPO–PEO (EP-0.33:1) | 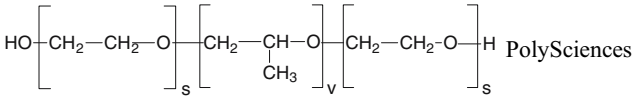 PolySciences | $M_w$=3,400 | 1.03 | 0.33:1 |
| PEO–PPO–PEO (EP-0.8:1) | | $M_w$=2,900 | 1.05 | 0.8:1 |
| PEO–PPO–PEO (EP-3:1) | | $M_w$=13,300 | 1.05 | 3:1 |

equipped with a Mettler EP2HF heating stage. Samples were placed between two glass slides. Cloud point times, $t_{cp}$, were determined as the time at which a decrease in the transmitted light intensity was recorded.

## Results and discussion

### EPOXY blends modified with homopolymers

Firstly, analysis of the mixtures containing PEO and PPO homopolymers has been carried out to understand the morphological evolution in epoxy matrices modified with different PEO-PPO-PEO block copolymers. Samples modified with different PEO contents and cured at different temperatures remained transparent and not phase separation was detected by AFM (not shown here), thus, suggesting miscibility in these systems.

Figure 1 shows FTIR spectra for DGEBA/DDM blends containing different PEO contents cured at 80 °C and postcured at 190 °C. The broad band centred at 3,527 $cm^{-1}$ is attributed to associated hydroxyl groups and the band centred around 3,559 $cm^{-1}$ is assigned to free hydroxyl groups. The associated hydroxyl group band shifts to lower frequencies as PEO content increases. Moreover, the intensity ratio between associated and free hydroxyl bands increase as the PEO content does. This fact suggests that the OH groups developed through cure reactions interact by hydrogen-bonding with the block copolymer –O– bonds. So, hydrogen-bonding interactions between the components of these mixtures lead to a miscible system [14, 15].

These blends have also been examined using dynamic mechanical analysis to get more information about the state of miscibility of DGEBA/DDM/PEO cured blends.

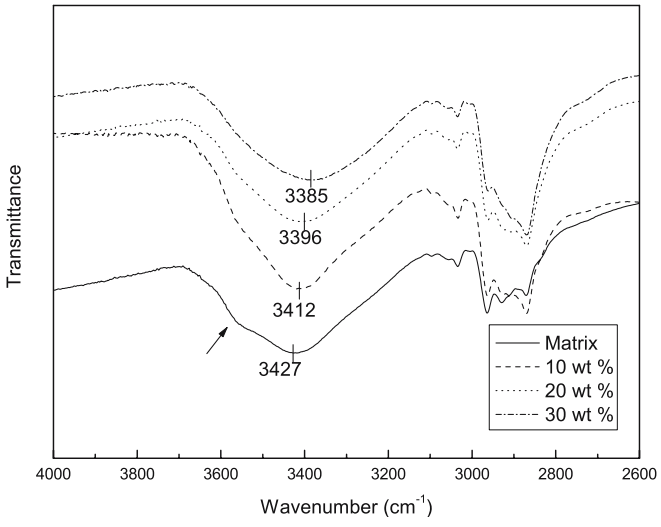


**Fig. 1** FTIR spectra for DGEBA/DDM blends containing different PEO contents. The samples were cured at 180 °C and postcured at 190 °C

Figure 2 shows storage modulus ($E'$) and tan $\delta$ variation with temperature for different PEO contents of samples cured at 80 °C and postcured at 190 °C. A single sharp tan $\delta$ peak that moved to lower temperatures as PEO content increased suggests that the mixtures are miscible [16].

On the contrary, macrophase separation induced by chemical reactions of the initially miscible system occurred in epoxy systems modified with different PPO contents as the samples were opaque. The morphologies of PPO modified systems at different cure temperatures and PPO contents are shown in Fig. 3a–c. As can be seen, all mixtures exhibited two different phases. Big particles of PPO dispersed in an epoxy-rich phase can be observed, their size being dependent on the cure temperature and PPO content.

FTIR spectra for these systems (Fig. 4) show that neither the associated hydroxyl group band nor the band assigned to free hydroxyl groups change with PPO content. This fact suggests that interactions between OH groups developed through cure reactions and PPO homopolymer are negligible. Dynamic mechanical analysis (DMA) carried out on samples cured at 80 °C and postcured at 190 °C is shown in Fig. 5. The macrophase separated structure is confirmed by the presence of the $\alpha$ relaxation of epoxy-rich phase close to that corresponding to the neat matrix.

### EPOXY blends modified with block copolymers

PEO–PPO–PEO modified epoxy blends containing 10, 20 and 30 wt% copolymer have been first visually analysed. Systems modified with EP-0.33:1 were opaque at all contents and cure temperatures, thus, suggesting the existence of a macrophase-separated structure in the blends. On the contrary, the system modified with EP-3:1 remained transparent even after postcuring at 190 °C. This fact could indicate the existence of a single homogeneous phase or a microphase separated structure. In the case of EP-0.8:1 modified system, the samples were opaque or transparent depending on the cure temperature. Similar results were obtained for other PEO–PPO–PEO block copolymers by Mijovic et al. [11] and Guo et al. [12].

Morphological analysis for block copolymer modified systems cured at 80 or 140 °C is shown in Figs. 6 and 7, respectively. The system modified with EP-3:1 presents microphase separated domains at both cure temperatures 80 °C, Fig. 6a.1–3, and 140 °C, Fig. 7a.1–3. On the other hand, EP-0.8:1 modified system shows miscible, macro- or microphase separated domains depending on cure temperature and copolymer content, Figs. 6b.1–3 and 7b.1–3 [4]. For 10 wt% modified system, the copolymer remained miscible or the microdomains were not discernible, Fig. 6b.1. When EP-0.8:1 content increased up to 20 wt% spherical micelles were formed, which remained coexisting with wormlike micelles for 30 wt% modified system (Fig. 6b.2 and b.3). Taking into account that EP-

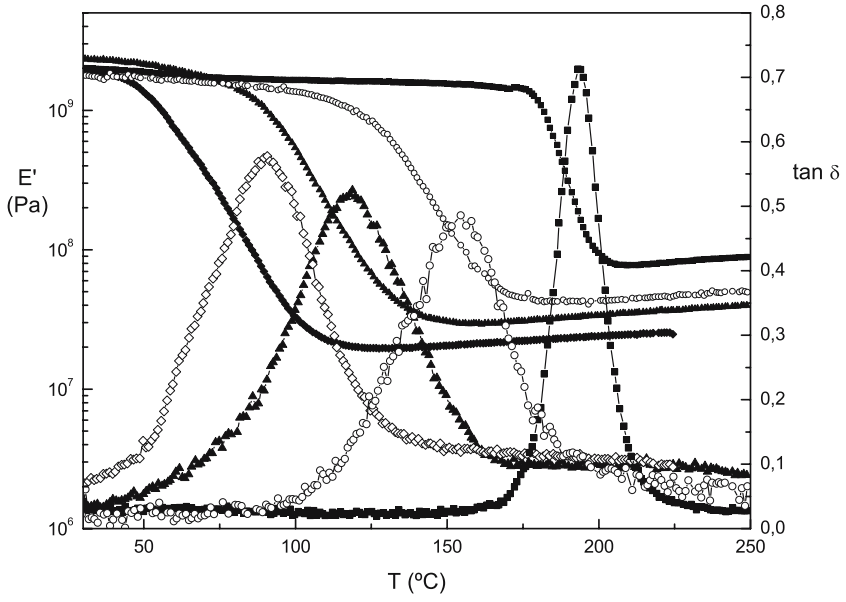


**Fig. 2** Storage modulus (E′) and loss factor (tan δ) variation upon temperature for (■) neat DGEBA/DDM system and its blends modified with different PEO contents: (○) 10 wt%, (▲) 20 wt%, and (◊) 30 wt%, cured at 80 °C and postcured at 190 °C

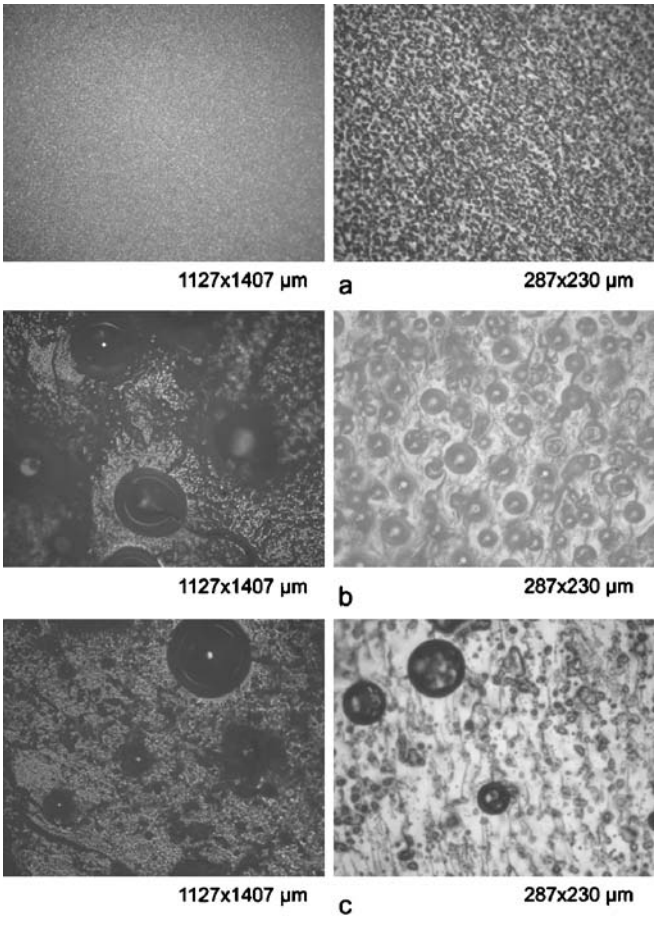


**Fig. 3** Optical microscopy images of DGEBA/DDM blends modified with different PPO contents: **a** 10 wt% and cured at 80 °C, **b** 20 wt% and cured at 80 °C, and **c** 20 wt% and cured at 140 °C. All samples were postcured at 190 °C

0.8:1 copolymer has a higher content of PPO than EP-3:1, phase separation should occur through cure. Nonetheless, it has a lower molecular weight PPO block than that corresponding to EP-3:1, which could make possible that for the system with 10 wt% copolymer cured at 80 °C, the mixture remained miscible without phase separation or perhaps forming very small micelles. For 140 °C cured samples, however, AFM images shown in Fig. 7b.1–3 evidence the macrophase separation at all contents. As discussed previously [4], DGEBA:DDM/EP-0.8:1 system shows low critical solution temperature (LCST) behaviour.

On the other hand, according to the opacity of the samples, AFM and OM images for EP-0.33:1 modified systems reveal macrophase separated domains for both

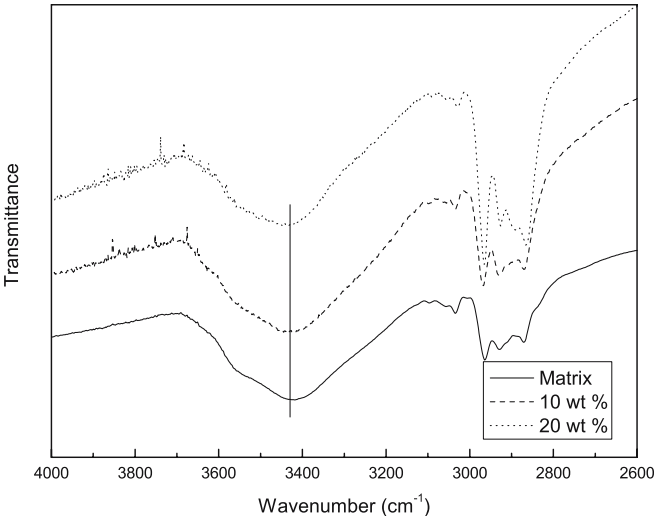


**Fig. 4** FTIR spectra for DGEBA/DDM blends containing different PPO contents. The samples were cured at 80 °C and postcured at 190 °C

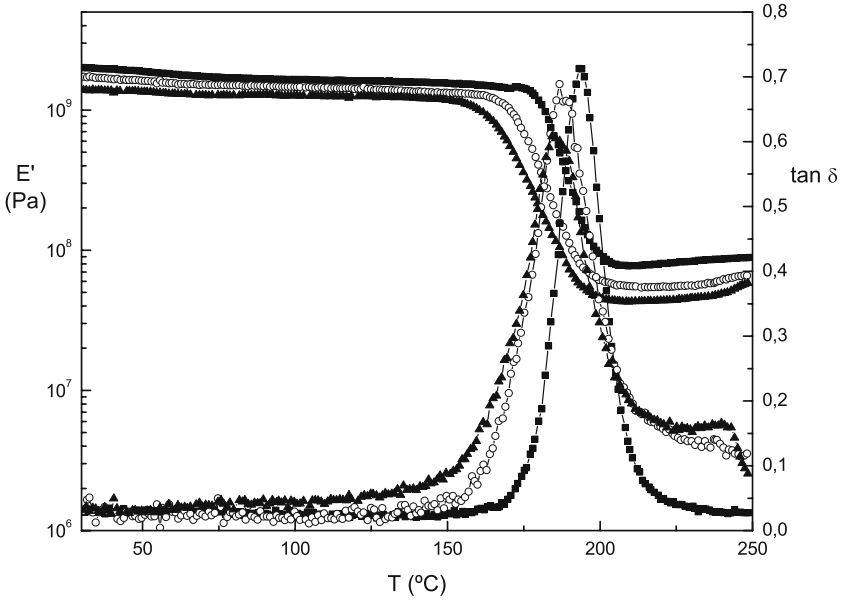


**Fig. 5** Storage modulus (E′) and loss factor (tan δ) variation upon temperature for (■) neat DGEBA/DDM system and its blends modified with different PPO contents: (○) 10 wt% and (▲) 20 wt%, cured at 80 °C and postcured at 190 °C

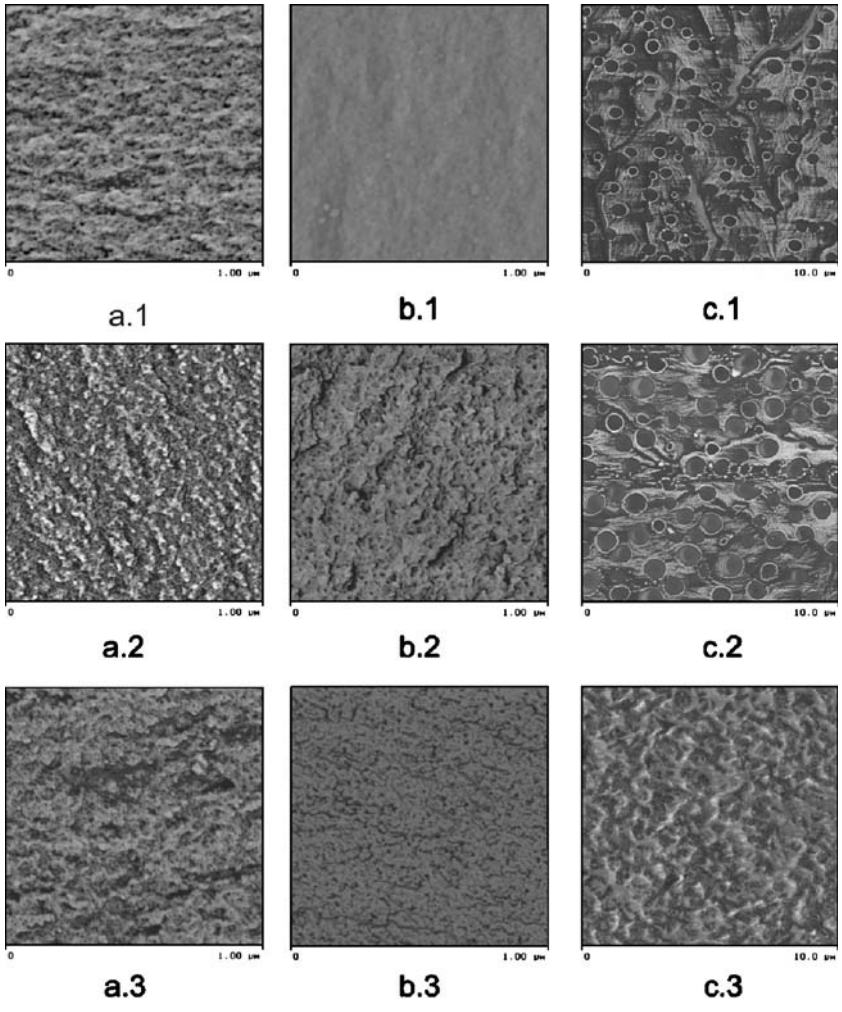


**Fig. 6** Phase TM-AFM images of DGEBA/DDM blends containing: **a** EP-3:1, **b** EP-8:1, and **c** EP-0.33:1 with different contents: *1* 10 wt%, *2* 10 wt% and *3* 30 wt%. Samples were cured at 80 °C and postcured at 190 °C

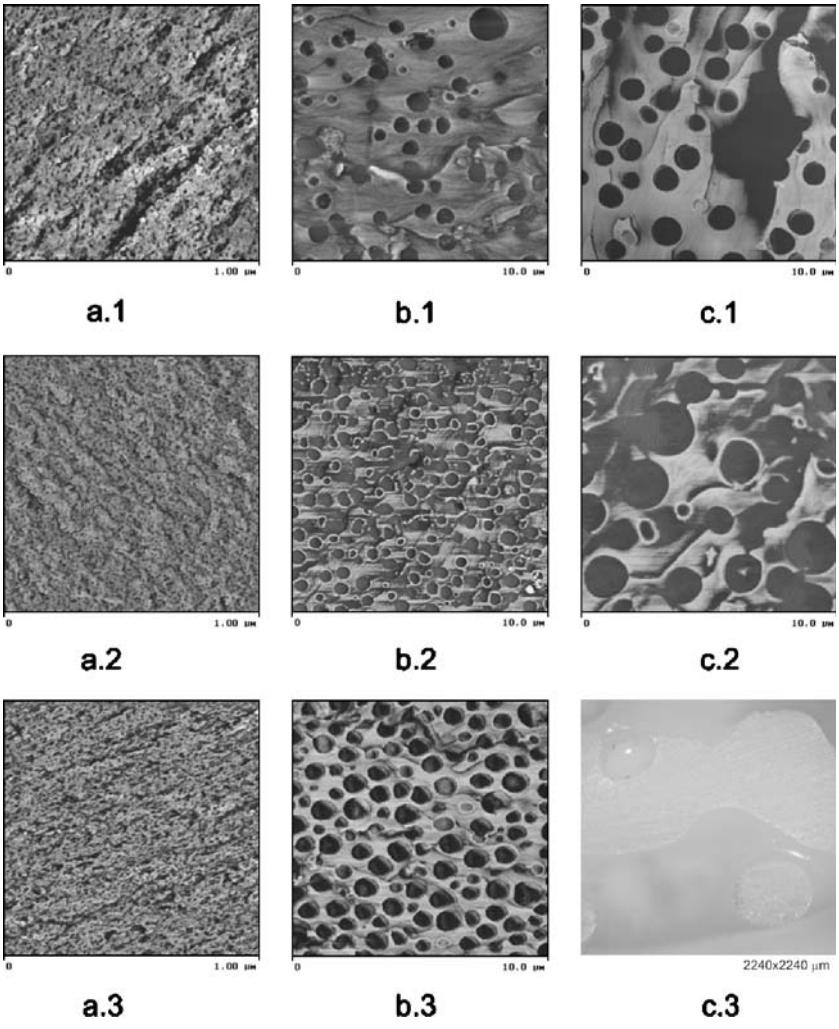


**Fig. 7** Phase TM-AFM or OM images of DGEBA/DDM blends containing: **a** EP-3:1, **b** EP-8:1, and **c** EP-0.33:1 with different contents: *1* 10 wt%, *2* 20 wt% and *3* 30 wt%. Samples were cured at 140 °C and postcured at 190 °C

80 °C and 140 °C cure temperatures, as shown in Figs. 6c.1–3 and 7c.1–3, respectively. Despite of the fact that PEO block is miscible with the thermoset matrix, the high content of PPO block, which is not miscible, led to macrophase separation because the interactions between PEO and epoxy matrix were not strong enough to stabilize the micelles at any cure temperature and copolymer content analysed. For blends containing 10 wt% EP-0.33:1 spherical domains, the size of which increased from around 350 and 550 nm up to around 550 and 1,100 nm with cure temperature (Figs. 6c.1 and 7c.1), have been observed. The system modified with 20 wt% EP-0.33:1 and cured at 80 °C shows particles at around 450, 650 and 850 nm diameter (Fig. 6c.2), which increased up to around 450, 1,000 and 1,700 nm as cure temperature increased up to 140 °C (Fig. 7c.2). As shown below, the system modified with EP-0.33:1 also presents LCST behaviour, so a decrease in cloud point conversion occurs as cure temperature increases. In addition, as viscosity is lower at higher temperature, its mobility is higher at the time of formation of macrophase separated structures and, consequently, growth and coalescence of the separated phase was favoured, which led to an increase in average diameter and a decrease in dispersed particles concentration. When the EP-0.33:1 content increased up to 30 wt%, different morphologies were developed depending on cure temperature: co-continuity for 80 °C (Fig. 6c.3) and phase inversion, where PEO–PPO–PEO-rich phase formed the matrix and the thermoset matrix appeared as big interconnected spherical domains, for samples cured at 140 °C (Fig. 7c.3).

A schematic representation of the self-assembling process for these blends is presented in Fig. 8. At the early state of cure the block copolymer was miscible with the epoxy system (I). As cure advanced, PPO block, which has enough molecular weight, self-assembled into nanoscopic entities (II) because of unfavourable interactions of PPO with epoxy, then leading to the formation of nanomicelles (III) in the cured blends. PEO possibly acted as a bridge between both separated phases. As observed by Dean [9, 10], Mijovic [11] and Guo [5, 12] in analogue systems, spherical domains of around 10-nm diameter were formed

at low copolymer contents for both cure conditions. Moreover, the amount of spherical micelles increased at higher copolymer contents. The mixture modified with 30 wt% EP-3:1 block copolymer self-assembled into spherical and wormlike micelles. The formation of microphase separated domains is due to the fact that one block remained miscible during the cure process, in the same way to that reported by Ritzenthaler et al. [2, 3]. The formation of these domains occurred through nucleation and growth mechanism, where the interactions between PEO and the forming epoxy network stabilized the formed nuclei.

To further investigate the morphological behaviour of blends with different block copolymers, dynamic mechanical analysis was carried out on the cured samples between room temperature and 250 °C. Figure 9 shows storage modulus and tan $\delta$ variation with temperature for DGEBA/DMM system modified with different PEO–PPO–PEO copolymers for different contents cured at 80 °C (Fig. 9a–b) and cured at 140 °C for 20 wt% (Fig. 9c). For comparison, DMA curves for PEO and PPO homopolymer modified systems have also been included. As shown above, PEO modified system was miscible with epoxy resin and PPO modified system macrophase separated. The microphase separated systems presented the $\alpha$ relaxation of epoxy-rich phase at temperatures between those for systems modified with the respective homopolymers. For 10 wt% block copolymer modified systems cured at 80 °C, Fig. 9a, the $\alpha$ relaxation of epoxy-rich phase appeared at different temperatures depending on PEO:PPO molar ratio. The similar temperature of $\alpha$ relaxation of epoxy-rich phase for EP-0.33:1 and PPO modified systems suggest macrophase separation. For EP-3:1 modified system, the $\alpha$ relaxation appeared to be intermediate between the corresponding ones to PPO and PEO modified systems, thus, indicating a higher extent of interactions between epoxy-rich phase and PEO blocks. For EP-0.8:1 modified system, however, the $\alpha$ relaxation was very similar to that corresponding to PEO modified system, suggesting miscibility or some microphase separation in this blend, which can be explained taking into account the low molecular weight of PPO block in this copolymer. The influence of cure temperature on 20 wt% modified systems can be analysed by comparing Fig. 9b and c.

Similar to that observed for 10 wt% EP-0.33:1 modified system, the $\alpha$ relaxation appeared to be nearly unaffected with respect to the system modified with PPO homopolymer at both temperatures. The system modified with EP-3:1 showed a $\alpha$ relaxation intermediate between those corresponding to systems modified with PPO and PEO homopolymers at both temperatures, thus, indicating a higher extent of interactions between epoxy-rich phase and PEO blocks. Moreover, for EP-0.8:1 modified system, the $\alpha$ relaxation appeared closer to that corresponding to PEO or PPO modified systems depending if cure temperature was 80 or 140 °C, respectively, which can be explained taking into account both the low molecular weight of PPO block and the LCST behaviour for this system. Therefore, DMA analysis confirms the formation of the different structures observed by AFM and OM analysis.

A thermodynamic approach for phase separation of DGEBA/DDM/EP-0.33:1 system, similar to that previously employed for EP-0.8:1 modified system [4], has been used to analyse the obtained morphologies. The thermodynamic model is based on the Flory–Huggins (F–H) equation [17]. For this analysis, the block copolymer has been considered as only one entity and the polydispersities of both PEO–PPO–PEO and thermoset component have been considered.

F–H equation to describe the free energy of mixing of two polydisperse polymers per mole of unit cell is given by

$$\frac{\Delta G^m}{RT} = \sum \frac{\phi_i}{Z_i} \ln \phi_i + \sum \frac{\phi_j}{Z_j} \ln \phi_j + \chi \phi_1 \phi_2 \qquad (1)$$

where $T$ is the absolute temperature (K), $Z_j = \frac{V_j}{V_r}$ and $Z_i = \frac{V_i}{V_r}$, the number of lattice sites occupied by $j$-mer (copolymer species) and $i$-mer (epoxy-amine species), respectively, being $V_i$ and $V_j$ the volume of the $i$-mer and $j$-mer, respectively, and $V_r$ the reference volume taken as the volume for the smallest species (DDM in this case). The volume fractions of reactive blend and copolymer are $\phi_1 = \sum_i \phi_i = \sum_m \sum_n \phi_{m,n}$ and $\phi_2 = \sum_j \phi_j$, respectively.

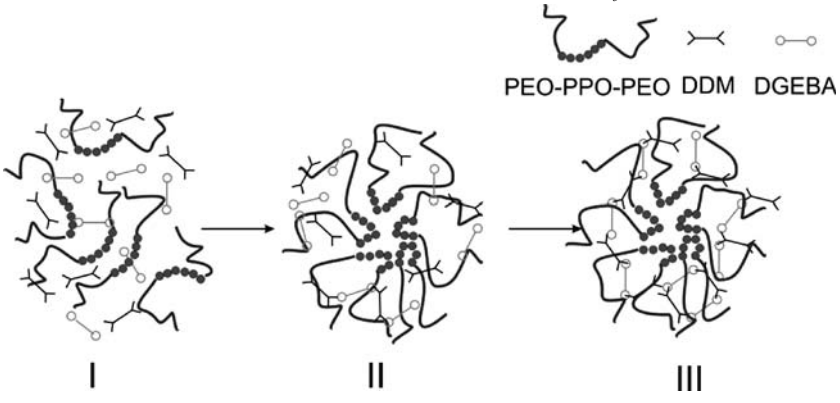


**Fig. 8** Schematic representation of formation of micellar type nanoseparated structures

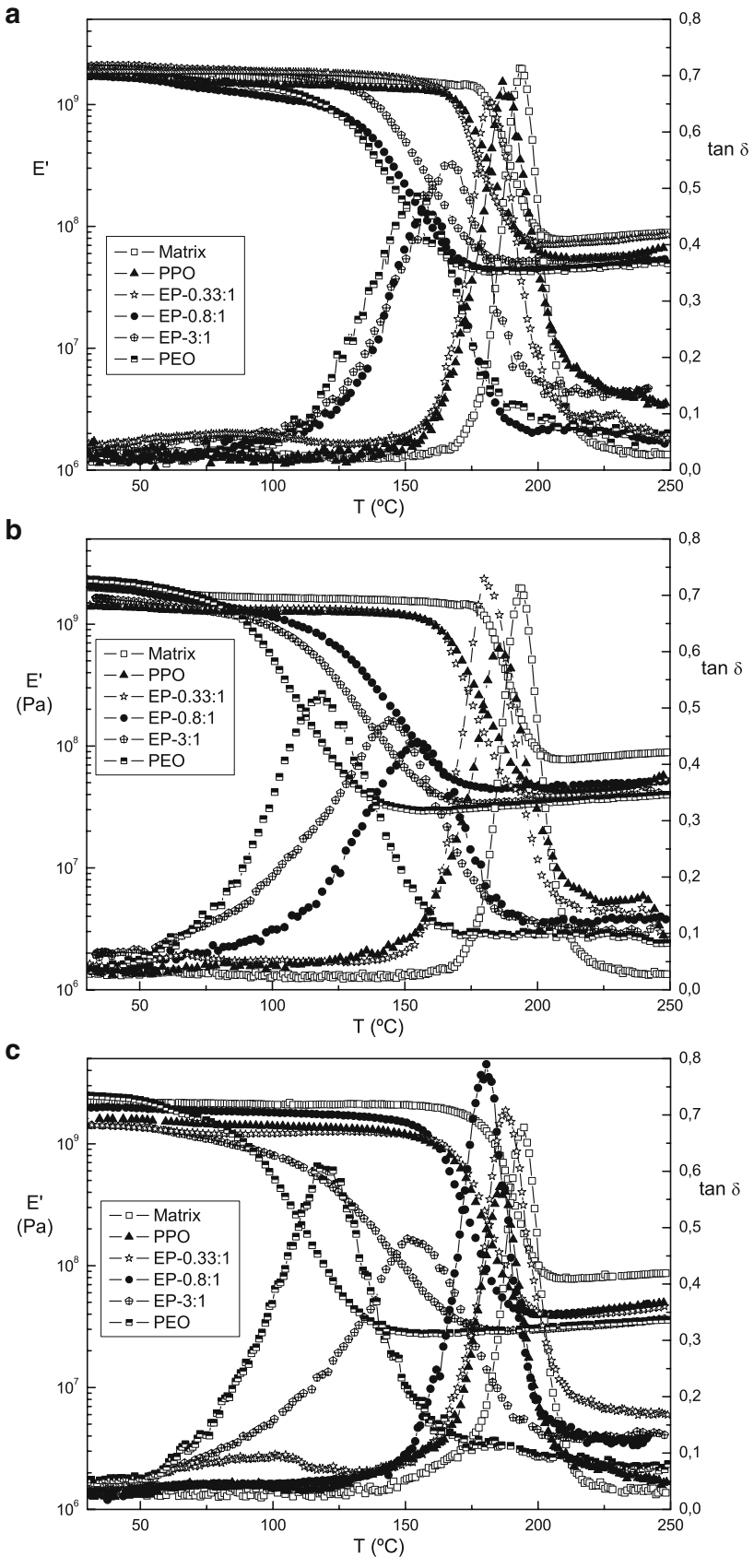


**Fig. 9** Storage modulus and loss factor (tan δ) variation upon temperature for neat matrix and blends containing PPO, block copolymers and PEO cured at **a** 80 °C, 10 wt%; **b** 80 °C, 20 wt% and **c** 140 °C, 20 wt%

$\phi_{m,n}$ is defined by $\phi_{m,n} = [E_{m,n}][mV_{DDM} + nV_{DGEBA}]$, where $m$ and $n$ are the molecules of DDM and DGEBA contained in the different species epoxy-amine formed during reaction, $E_{m,n}$, and $|E_{m,n}|$ is the molar concentration of $E_{m,n}$ species.

The molecular weight distribution of PEO–PPO–PEO was calculated experimentally by GPC (not shown here), which is necessary to know the volume of $j$-mer. The distribution of epoxy-amine species formed during reaction at an overall conversion $X$, which is necessary to know the volume of $i$-mer, is given by the Stockmayer distribution function [18, 19]. Thus, molar concentration of $E_{m,n}$ can be described as $[E_{m,n}] = [A]_0 \frac{4(3m)!X^{m+n-1}(1-X)^{2m+2}}{m!(3m-n+1)!(n-m+1)!}$ where $[A]_0$ is the initial molar concentration of DDM in the blend [20–23].

By using cloud point times of the macrophase separated blends and curing kinetic curves (Larrañaga et al., submitted for publication), cloud point conversions can be obtained for each percentage of block copolymer in the blend. These data allow knowing the molar concentration of epoxy-amine species at the cloud point time.

As shown in the following paragraphs, through the derivation of Gibb's free energy per mol of each component ($n$), it is now possible to calculate the $\chi$ parameter for each temperature and composition:

$$\Delta\mu_i = \left.\frac{\partial \Delta G^m}{\partial n_i}\right|_{P,T,n_{k\neq i}} \tag{2}$$

$$\frac{\Delta\mu_i}{RT} = 1 + \ln\phi_i - Z_i\left[\left(\frac{\phi_1}{\overline{Z_1}} + \frac{\phi_2}{\overline{Z_2}}\right) - \chi\phi_2^2\right] \tag{3}$$

and

$$\frac{\Delta\mu_j}{RT} = 1 + \ln\phi_j - Z_j\left[\left(\frac{\phi_1}{\overline{Z_1}} + \frac{\phi_2}{\overline{Z_2}}\right) - \chi\phi_1^2\right] \tag{4}$$

where

$$\frac{\phi_1}{\overline{Z_1}} = \sum_i \frac{\phi_i}{Z_i} \tag{5}$$

and

$$\frac{\phi_2}{\overline{Z_2}} = \sum_j \frac{\phi_j}{Z_j} \tag{6}$$

At the equilibrium of the $\alpha$ and $\beta$ phases,

$$\Delta\mu_i^\alpha = \Delta\mu_i^\beta \tag{7}$$

$$\Delta\mu_j^\alpha = \Delta\mu_j^\beta \tag{8}$$

Also, by applying Eqs. 4 and 7,

$$\frac{1}{Z_i}\ln\frac{\phi_i^\beta}{\phi_i^\alpha} = \left(\frac{\phi_2^\beta}{\overline{Z_2}^\beta} + \frac{\phi_1^\beta}{\overline{Z_1}^\beta}\right) - \left(\frac{\phi_2^\alpha}{\overline{Z_2}^\alpha} + \frac{\phi_1^\alpha}{\overline{Z_1}^\alpha}\right) + \chi\left(\phi_2^{\alpha^2} - \phi_2^{\beta^2}\right) \tag{9}$$

replacing Eqs. 5 and 8, we obtain

$$\frac{1}{Z_j}\ln\frac{\phi_j^\beta}{\phi_j^\alpha} = \left(\frac{\phi_2^\beta}{\overline{Z_2}^\beta} + \frac{\phi_1^\beta}{\overline{Z_1}^\beta}\right) - \left(\frac{\phi_2^\alpha}{\overline{Z_2}^\alpha} + \frac{\phi_1^\alpha}{\overline{Z_1}^\alpha}\right) + \chi\left(\phi_1^{\alpha^2} - \phi_1^{\beta^2}\right) \tag{10}$$

$\sigma_1$ and $\sigma_2$ are defined by

$$\sigma_1 = \frac{1}{Z_i}\ln\frac{\phi_i^\beta}{\phi_i^\alpha} \tag{11}$$

and

$$\sigma_2 = \frac{1}{Z_j}\ln\frac{\phi_j^\beta}{\phi_j^\alpha} \tag{12}$$

By introducing Eqs. (5, 6, 11, and 12) in Eqs. (9 and 10), the following equations are obtained:

$$\sigma_1 - \left(\sum_j \frac{\phi_j^\beta}{Z_j} + \sum_i \frac{\phi_i^\beta}{Z_i}\right) + \left(\sum_j \frac{\phi_j^\alpha}{Z_j} + \sum_i \frac{\phi_i^\alpha}{Z_i}\right) - \chi\left(\left(\sum_j \phi_j^\alpha\right)^2 - \left(\sum_j \phi_j^\beta\right)^2\right) = 0 \tag{13}$$

and

$$\sigma_2 - \left(\sum_j \frac{\phi_j^\beta}{Z_j} + \sum_i \frac{\phi_i^\beta}{Z_i}\right) + \left(\sum_j \frac{\phi_j^\alpha}{Z_j} + \sum_i \frac{\phi_i^\alpha}{Z_i}\right) - \chi\left(\left(\sum_i \phi_i^\alpha\right)^2 - \left(\sum_i \phi_i^\beta\right)^2\right) = 0 \quad (14)$$

By Eqs. (11 and 12), the following ones are obtained

$$\phi_i^\beta = \phi_i^\alpha \exp(\sigma_1 Z_i) \quad (15)$$

and

$$\phi_j^\beta = \phi_j^\alpha \exp(\sigma_2 Z_j) \quad (16)$$

At the beginning of the phase separation process, the composition of the α phase is the initial one, $\phi_1^\alpha = \phi_{1,0}$ and $\phi_2^\alpha = \phi_{2,0}$ by the distribution of modifier, we obtain

$$\phi_j = w_j \phi_2$$

where $w_j$ is the mass fraction of $j$ species of 2 polymer, so

$$\phi_j^\alpha = w_j \phi_{2,0}$$

The composition of the β phase fulfils the balance,

$$\phi_1^\beta + \phi_2^\beta - 1 = 0 \quad (17)$$

In this system, three unknown quantities, $\sigma_1$, $\sigma_2$ and $\chi$, exist, and three nonlinear equations, Eqs. (12, 13 and 17), are needed. The resolution of this system is done with the numerical method of Newton Raphson.

So that, for this model, the interaction parameter has been calculated as a function of conversion and cure temperature. The obtained dependences with temperature and conversion for EP-0.33:1 and EP-0.8:1 modified systems [4] are $\chi = 1.04 - \frac{310+72X}{T}$ and $\chi = 3.25 - \frac{1400-215X}{T}$, respectively.

LCST behaviour can be observed in $\chi$, expressions, as they are $a - \frac{b}{T}$ type.

Introducing $\chi$ expression in Eqs. (13 and 14) and taking into account Eq. (17), it is possible to know $\sigma_1$, $\sigma_2$ and $T$. From these parameters, composition vs temperature profiles can be obtained at different conversions. So that, it becomes possible to represent theoretical cloud point times (which are related with conversion by kinetic curves) vs composition at each temperature.

Figure 10 shows the results for DGEBA/DDM/EP-0.33:1 system at each cure temperature, where plots of experimental values of cloud times vs volumetric fraction of modifier are compared with those calculated by the thermodynamic model used. Similar to that observed for DGEBA/DDM/EP-0.8:1 system [4], the predicted cloud point times fits quite well with the experimental data at all compositions and cure temperatures are analysed.

The F–H model has been used to analyse the different morphologies. Generally speaking, the final morphologies of thermosetting systems modified with polymers are a result of the competition between the rate of phase separation from an initial homogeneous miscible mixture and gelation (polymerization reaction). When macrophase separation happens, it takes place during the period comprised between cloud point and gelation [24–26]. The critical point at which the binodal curve shows a minimum in temperature (critical temperature, $T_c$) for LCST behaviour, is displaced to lower temperatures as conversion increases through curing of the epoxy matrix. Therefore, for high cure temperatures, the critical point conversion is lower, and consequently, the mixture has enough conversion interval up to the occurrence of gelation to develop phase-separated morphologies. On the contrary, at lower cure temperatures, mixtures move to the immiscibility region of the phase diagram at higher conversions, and thus, the conversion interval after phase separation up to gelation becomes lower. As a consequence, phase separation even cannot happen at low cure temperatures.

By using the equations proposed by Koningsveld and Kleintjens for polydisperse systems [27], the ratio of the critical interaction parameter and also the critical composition upon critical conversion has been deduced. By introducing this ratio in the above equations that relate

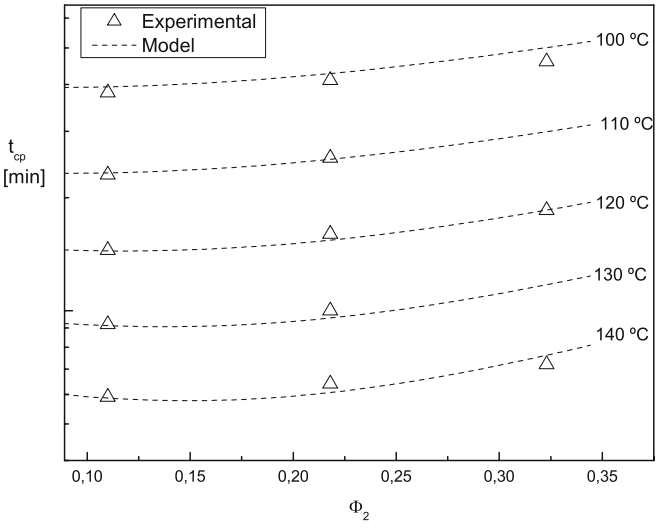


**Fig. 10** Experimental (8) and predicted cloud point time (---) for DGEBA/DDM blends modified with different EP-0.33:1 contents

the interaction parameter with temperature, the critical temperature can be calculated. Figure 11 presents the variation of the conversion corresponding to the critical point upon the critical temperature for the system modified with EP-0.33:1, also including the conversion to gelation, $X_g$, determined by Matijka and Dušek for DGEBA/DDM system [28]. As this conversion value is lower than $X_g$ for both cure temperatures used in this work, phase separation will occur for all amounts of block copolymer in the mixtures.

Table 2 shows theoretical critical temperatures for EP-0.33:1 and EP-0.8:1 modified systems. The location of $T_c$ with respect to the cure temperature used for each initial mixture composition [29] is the most important factor controlling the morphologies generated. The model predicts $T_c$ higher than 140 °C for both 10 and 20 wt% EP-0.33:1 modified systems, which is far away from both cure temperatures used. Indeed, those predictions indicate particulated morphologies for both cure temperatures as the critical point is displaced to higher conversions as chemical reactions take place. Nonetheless, when copolymer content increases up to 30 wt%, $T_c$ decreases up to 95 °C, which is intermediate between both cure temperatures used. Thus, different morphologies should be presented depending on cure conditions, co-continuous at 80 °C due to the near $T_c$ and phase inverted at 140 °C due to it lower than $T_c$. In the case of 10 and 20 wt% EP-0.8:1 modified systems, $T_c$ is higher than 170 °C, which agree with the particulated morphology observed for these systems cured at 140 °C. Nevertheless, the system modified with 30 wt% EP-0.8:1 shows a $T_c$ of 145 °C suggesting co-continuous or inverted morphologies, which do not agree with experimental results. This can be due to the fact that block copolymer has been considered as only one entity and, consequently, the interactions between block copolymer and epoxy resin have not been taken into account in the thermodynamic model used.

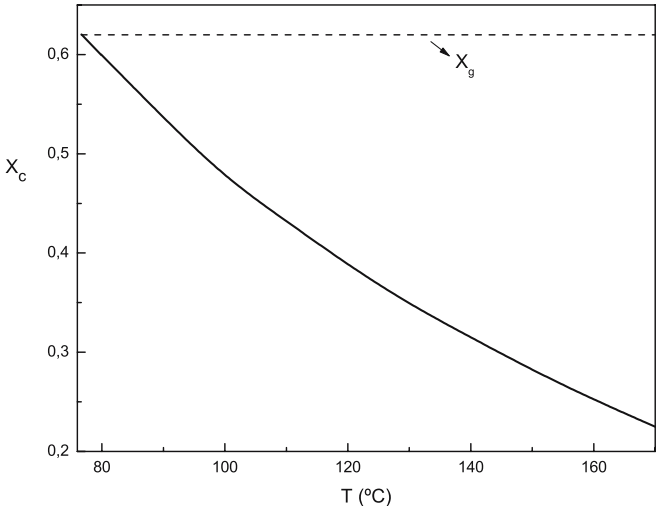


**Fig. 11** Critical conversion as a function of temperature for EP-0.33:1 modified system (—) and gel-point conversion of neat DGEBA/DDM system (---)

## Conclusions

Microphase separation induced by self-assembling of thermoset systems modified with block copolymers can be achieved by blending and curing a DGEBA/DDM system with PEO–PPO–PEO block copolymers. Macro- or microseparated structures can be systematically designed depending on: molar ratio between blocks, molecular weight of blocks, cure temperature and content of block copolymer.

For high PEO:PPO molar ratio, microphase separated structures have been obtained at all block copolymer contents and cure temperatures used. It has been proved that physical interactions between thermoset and PEO block occur during cure process, thus, avoiding PEO phase separation whilst PPO block tends to separate from thermoset. Therefore, PPO block can self-assemble into nanoscopic entities; those can be stabilized as micelles by those physical interactions, thus, avoiding their coalescence, and consequently, the macrophase separation process. Moreover, spherical or wormlike micelles can be obtained depending on copolymer content.

At low PEO:PPO molar ratio, physical interactions of PEO block with the epoxy matrix are not enough favourable due to the lower content of PEO block. Indeed, the micelles formed initially coalesce leading to macroscopic phase separation, where different morphologies are obtained depending on copolymer content and cure temperature.

For intermediate PEO:PPO molar ratio, the structural features of the mixtures are function of both copolymer content and cure temperature. At high cure temperature, the micelles cannot be stabilized due to the initial low viscosity, and so, they coalesce forming macrophase separated domains. Nonetheless, at low cure temperatures the interactions between PEO and epoxy matrix are able to stabilize micelles. Moreover, at low block copolymer contents the systems remain miscible due to the low molar mass of PPO block.

Thus, a rational design of thermosetting epoxy matrices structured at nanoscale can be obtained by controlling

**Table 2** Predicted critical temperatures vs block copolymer content for EP–0.33:1 and EP–0.8:1 modified systems

| Block copolymer content (wt%) | $T_c$ (°C) | |
|---|---|---|
| | DGEBA/DDM/ EP-0.33:1 | DGEBA/DDM/ EP-0.8:1 |
| 10 | >170 | >170 |
| 20 | 160 | 170 |
| 30 | 95 | 145 |

molar ratio and molecular weight of PEO–PPO–PEO block copolymers and also cure conditions. Potential applications of optically transparent nanoporous materials based on epoxy matrices could be developed through the use of these systems.

**Acknowledgements** Funding for this work was provided by Ministerio de Ciencia y Tecnología (Spain) Grants MAT1998-0656, MAT2000-0293 and MAT2001-0714. M. Larrañaga acknowledges financial support (grant for Ph.D.) from the Ministerio de Ciencia y Tecnología. C.C. Riccardi also thanks Gobierno Vasco/Eusko Jaurlaritza for the financial support for a sabbatical year.

## References

1. Hillmyer MA, Lipic PM, Hajduk DA, Almdal W, Bates FS (1997) J Am Chem Soc 119:2749
2. Ritzenthaler S, Court F, David L, Girard-Reydet E, Leibler L, Pascault JP (2002) Macromolecules 35:6245
3. Ritzenthaler S, Court F, Girard-Reydet E, Leibler L, Pascault JP (2003) Macromolecules 36:118
4. Larrañaga M, Gabilondo N, Kortaberria G, Serrano E, Remiro PM, Riccardi CC, Mondragon I (2005) Polymer 46:7082
5. Guo Q, Thomann R, Gronski W, Staneva R, Ivanova R, Stühn B (2003) Macromolecules 36:3635
6. Ruzette AV, Leibler L (2005) Nature Mater 4:19
7. Grubbs RB, Dean JM, Broz ME, Bates FS (2000) Macromolecules 33:9522
8. Lipic PM, Bates FS, Hillmyer MA (1998) J Am Chem Soc 120:8963
9. Dean JM, Lipic PM, Grubbs RB, Cook RF, Bates FS (2001) J Polym Sci: Part B: Polym Phys 39:2996
10. Dean JM, Verghese NE, Pham HQ, Bates FS (2003) Macromolecules 36:9267
11. Mijovic J, Shen M, Sy JW, Mondragon I (2000) Macromolecules 33:5235
12. Guo Q, Thomann R, Gronski W, Thurn-Albrecht T (2002) Macromolecules 35:3133
13. Serrano E, Martin MD, Tercjak A, Pomposo JA, Mecerreyes D, Mondragon I (2005) Macromol Rapid Commun 26:982
14. Guo Q, Harrats C, Groeninckx G, Koch MHJ (2001) Polymer 42:4127
15. Zhong Z, Guo Q (1998) Polymer 39:517
16. Zheng S, Zhang N, Luo X, Ma D (1995) Polymer 36:3609
17. Flory PJ (1953) Principles of Polymer Chemistry. Cornell University Press, Ithaca, New York
18. Stockmayer WH (1952) J Polym Sci 9:69
19. Stockmayer WH (1953) J Polym Sci 11:424
20. Riccardi CC, Borrajo J, Williams RJJ, Gyrard-Reydet E, Sautereau H, Pascault JP (1996) J Polym Sci: Part B: Polym Phys 34:349
21. Riccardi CC, Borrajo J (1993) Polym Int 3:241
22. Riccardi CC, Borrajo J, Maynie L, Fenouillot F, Pascault JP (2004) J Polym Sci: Part B: Polym Phys 42:1351
23. Bonnaud L, Bonnet A, Pascault JP, Sautereau H, Riccardi CC (2002) J Appl Polym Sci 83:1385
24. Remiro PM, Riccardi CC, Corcuera MA, Mondragon I (1999) J Appl Polym Sci 74:772
25. Chen JL, Chang FC (1999) Macromolecules 32:5348
26. Stefani PM, Riccardi CC, Remiro PM, Mondragon I (2001) Polym Eng Sci 41:2013
27. Koningsveld R, Kleintjens LA (1977) J Polym Sci: Part C: Polym Symp 61:221
28. Matìjka L, Dušek K (1991) Polymer 32:3195
29. Girard-Reydet E, Sautereau H, Pascault JP, Keates P, Navard P, Thollet G, Vigier G (1998) Polymer 39:2269